Atmospheric
Chemistry
and Physics

Supplement of

Carbon dioxide and methane measurements from the Los Angeles Megacity Carbon Project – Part 1: calibration, urban enhancements, and uncertainty estimates

Kristal R. Verhulst et al.

Correspondence to: Kristal R. Verhulst (kristal.r.verhulst@jpl.nasa.gov)

In this document, we describe: (1) Data acquisition and QA/QC protocols; (2) the "Alternate Calibration Method," which is a correction applied to the air data from La Jolla and Victorville using a 2-point calibration method; (3) Data selection criteria and curve fitting parameters for the CCGCRV software used to estimate background; (4) Estimates of epsilon (the slope component of the extrapolation uncertainty) for CO_2 and CH_4 based on laboratory measurements using CRDS analyzer units similar to those deployed in the field; (5) Uncertainty due to permeability of the Nafion drier determined from laboratory experiments; (6) Results from an Allan deviation analysis conducted using daily calibration runs from the La Jolla analyzer during January 2016; (7) Example plots showing the CO_2 and CH_4 calibration baseline uncertainty using three possible time series of Picarro sensitivity for the standard tank measurements from the La Jolla site during January 2016; (8) Results for the uncertainty associated with background (U_{BG}) for the San Clemente Island, Victorville, and La Jolla estimates.

1) Data Acquisition and Quality Control

1.1) Data acquisition

The LA in situ network includes sites deployed by Earth Networks, Inc. (http://www.earthnetworks.com/OurNetworks/GreenhouseGasNetwork.aspx). The GCWerks software manages the data flow. This software was originally developed for use in the Advanced Global Atmospheric Gases Experiment (AGAGE) network to provide a secure point of access to acquire data from remote instruments and has since been adapted for data management of CRDS analyzers using a Linux-based system (http://www.gcwerks.com). GCWerks also assists in the operation of the LA Megacity sites by reporting instrument diagnostics, sending user defined email alarms, applying pre-defined automated filter and flagging criteria to remove data impacted by instrument errors, and allowing graphical display of results. Several instrument diagnostics and quality control parameters including pressures, flow rates, cycle time, cavity pressure and cavity temperature are monitored in GCWerks to track the instrument status and measurement quality. The calibration correction (using the default, single-point calibration method) is also applied by GCWerks based on daily runs of the calibration standard tank (see Section 2 of the manuscript).

A master copy of GCWerks stored on the EN server ingests and merges the high-frequency CRDS greenhouse gas mole fractions and meteorological data, as well as the calibration information, port assignments, tank assignments, etc., on an hourly basis. The imported data are stored as binary strip-chart files, which are over 30 times smaller than the hourly Picarro files for fast data processing and copying. Metadata associated with the LA measurement sites is also stored and maintained on the EN server, including the most current versions of the ports.log and standards files. The standards file contains all the information about the assigned calibration tank values. The ports.log indicates the assignments for each of the air inlets and calibration standards, as well as the time period to reject before calculating averaged values from the native resolution Picarro data. Daily Picarro results are exported into yearly .csv files, which are checked offline against the standards files for additional updates (e.g., calibration tank assignments and data that requires manual flagging). Remote copies of GCWerks are also run by

site operators for data exploration via VNC connection.

1.2) Data quality control and automated filters

GCWerks applies some basic automated quality control flags, which filter and/or reject some of the Level 0 data points. We apply automated filters to the high-frequency data in GCWerks before subsequent processing.
Filtered data are displayed in GCWerks and are configured in the gcwerks.conf file. The filter criteria are listed in Table S1 and apply to individual high-resolution data points (letter codes: P, S, W, C, T).

Some data are also rejected to account for the stabilization period after the inlet is switched. The first 10 minutes of data are excluded from further analysis after switching from a calibration tank to an air inlet and the first minute is excluded when switching between air inlets. This allows for flushing time for the tank regulator and plumbing and stabilization of the measurement after valve switching. Data that is automatically or manually flagged or rejected data are also displayed in GCWerks with letter codes (F= flagged data and x = rejected data).

Manual data flagging is occasionally needed to ensure good quality control of the greenhouse gas data (e.g., to ensure the flags were applied correctly in the previous step, or to address technical issues or instrument errors that are outside the scope of the automated filters, such as when a field technician visits the site and impacts the regular sampling protocol). After automated filters are applied, the data are screened manually using a parameter called N filtered in GCWerks to identify instances where automated filters have been applied. Manual data flags are applied by Earth Networks based on recommendations from the LA Megacity Data Working Group, a team of scientists from NASA's Jet Propulsion Laboratory, Scripps Institution of Oceanography, the National Institute of Standards and Technology, and Earth Networks. Manual flags are applied on a case-by-case basis. The decision to flag the data is usually based on information or observations that suggest instrument issues. Many of these cases include technician site visits that require modifications to the plumbing on the instrument of calbox. For example, when a calibration standard is replaced or if an analyzer is removed and/or replaced during repair, room air may enter the instrument, which is not of scientific interest. In some instances, we identify problematic by first looking for large deviations in the cavity pressure, sample pressure, inlet pressure, and/or in the measured mole fraction data and then comparing the data alongside notes from technician logs. The numerous parameters monitored by GCWerks help narrow down the cause of anomalous observations. The N filtered parameter is also monitored and cases where a large number of data have been filtered are analyzed in more detail to determine if additional manual flags are required. The manual flags are applied on the EN server to indicate those data that are not recommended for further scientific evaluation or interpretation within the scope of the project.

The corrected data is generated by GCWerks at 1-minute average intervals and generated as a .csv file for export and further analysis outside of the GCWerks framework. These .csv report files are uploaded to a primary Earth Networks/GCWerks server and are synced nightly and later used to compute the hourly average (Level 3) product.

We primarily discuss the 1-hour average CO_2 and CH_4 air observations in Sections 3 and 4, which are from individual inlet heights (for tower sites), and from a combination of the 4 corner inlets (for rooftop sites). These hourly average data are a Level 3 product, which is averaged from the uncorrected (2-5 s) Picarro data. For rooftops, we used a method similar to McKain et al. (2015) to calculate the 1-hour average air observations using only "upwind" observations (determined from the 1-minute average data). Additionally, we used wind speed and direction observations to verify the "upwind" side of the building. We constructed an "upwind" index for each 1-minute CO_2 or CH_4 observation. The measurement was determined to be "upwind" if the building corner had the highest wind speed and the wind direction also corresponded to the same side of the building.

2) Alternate calibration method

An "Alternate Calibration Method" was explored using a linear fit between two tanks (one "near-ambient" tank and one ''high concentration" standard tank) where data was available. Each calibration run is used to derive a slope and intercept, which are then interpolated in time:

Xcorr alternate $=m*X'_{air} + b$ (Eq. S1)

where the slope m and intercept b. The Alternate Calibration Method uses the high concentration standard to determine the slope, m, and intercept, b, while the default (single-point calibration) method assumes a zero reading at zero measurement. Therefore, the Alternate Method becomes equivalent to the default calibration method if b = 0 and the slope m does not vary with mole fraction, so that m = 1/S for all points. Both methods of calibration assume linearity, in that the slope m (or 1/S), is a constant over all mole fractions.

Air data from the LJO and VIC sites were corrected using the two methods to quantify the effect of different calibration methods on the final air mole fraction data. Both of these sites had limited measurements of a high mole fraction (span) tank available at the time of this study. Figures S2 and S3 show the difference in air data from the LJO analyzer corrected with the 2-point calibration method and the single-point calibration method for CO_2 (upper panels) and CH_4 (lower panels). Figure S3 shows similar results for air data collected from the VIC analyzer. Overall, the single-point calibration method underestimates the CO_2 levels by about 0.2 ppm out of 100 ppm and underestimates the CH_4 levels by about 6 ppb out of 6000 ppb, or about 1 part in 1000 for the LJO site (Figure S2). The results were similar when the same analysis was performed using air data from the VIC analyzer (Figure S3).

3) Background selection criteria and curve fitting parameters for CCGCRV

Our data selection criteria for CO_2 loosely follow the discussion in Thoning *et al.* (1989), but differ slightly for the LA sites. As described in the text, our data selection approach relies on several criteria: (1) a small degree of variability within a one hour period, and 2) small hour-to-hour variability, and (3) persistence of the first two conditions for several hours. Based on these criteria, we exclude observations that are impacted by local emissions or recirculation effects. The selection criteria for SCI were as follows: (1) First, check for stability of the CO_2 and CH_4 observations within 1-hour and retain measurements if the 1-hour SD is <0.3 ppm CO_2 and <3 ppb CH_4; (2)

3

Next, find small hour-to-hour changes in CO_2 concentration and retain measurements if the hour-to-hour difference is less than 0.25 ppm CO_2. No hour-to-hour criteria were used for CH_4; (3) Finally, retain only those observations with several (6 or more) consecutive hours that meet criteria 1 and 2.

To determine the filter criteria, we first evaluated the standard deviation of the one hour average observations (Figure S4). During 2015, 70%, 42%, and 30% of the data had a one hour S.D. <0.3 ppm CO_2, 67%, 57%, and 42% of the data had a one hour S.D <3 ppb CH_4 filter criteria, and 60%, 35%, and 29% of the data met both criteria for the SCI, VIC, and LJO sites, respectively. We began by applying these criteria to all 3 sites since a significant fraction of the data were within these limits. Next, we chose the hour-to-hour stability cutoff (0.25 ppm CO_2) based on Thoning *et al.* (1989). For the final criteria, we performed several tests by setting the number of consecutive hours between 3 and 6 hours and analyzing the remaining observations.

We found that the LJO and VIC observations were most sensitive to the filter parameters, especially the hour-to-hour stability and number of consecutive hours (criteria 2 and 3). For VIC, we found that requiring 6 or more consecutive hours of stable conditions resulted in large data gaps over the entire season during summer months, making the background estimate highly uncertain during this period. After several adjustments to the filter criteria, we were able to reduce the gaps in the VIC background observations to <1 month by applying the following changes: 1) increasing the hour-to-hour stability from 0.3 ppm CO_2 to 0.5 ppm CO_2 and 2) decreasing the number of consecutive hours with stable conditions from six hours to four hours. For LJO, the original filter criteria did not produce large gaps (>1 month). Furthermore, increasing the allowable hour-to-hour stability or decreasing the number of consecutive hours resulted in a few anomalously high CO_2 and/or CH_4 observations being included in the result, which is unfavorable (and likely due to a persistent polluted air mass passing over the site rather than clean background air). For these reasons, we applied the same criteria at LJO and SCI.

We have considered possible impacts of PBL growth on the background analysis. As described in the main text, we use only nighttime flask samples for the MWO background estimate because this site is more sensitive to the LA Basin during daylight hours due to growth of the PBL and upslope winds. However, our filtering criteria for SCI, LJO, and VIC do not account for diurnal variations, e.g., due to variations in the planetary boundary layer height or due to potential daytime drawdown of CO_2 due to photosynthetic uptake. Initially, we made plots of the monthly average diurnal variability for the SCI, LJO, and VIC sites. However, it was not apparent how the diurnal cycle would aid in the interpretation of background because most of the time the diurnal changes at these sites are dominated by impacts from local emissions (especially at LJO and to a lesser extent at the other two background sites due to outflow). At the marine background sites (LJO and SCI), it is the growth the marine boundary layer (MBL) rather than the PBL over the land, that is relevant to the interpretation of background. However, the MBL growth effect is most relevant when a site located very far off-shore, such that nighttime continental outflow is not present. Under these conditions, changes in the MBL with time of day are likely to be very small. The LJO is near sea level and is within the MBL, but is frequently impacted by local sources. The SCI site can be either within or above the MBL due to its elevation (~489 m asl), but is still occasionally impacted by continental outflow. For these reasons, we do not limit the background consideration to certain times of day. The agreement between the SCI

and LJO marine background estimates (within $\sim\pm1$ ppm CO_2 and $\sim\pm10$ ppb CH_4) suggests that there is not a large gradient between the CO_2 and CH_4 levels in the surface MBL and above the MBL. In summary, for the SCI, LJO, and VIC background sites, our underlying assumption is that if the PBL (or MBL) grows, it will not further dilute the CO_2 or CH_4 levels or cause additional large variations if the site is truly sampling background conditions.

5   After applying the selection criteria respective to each site, the CCGCRV curve fitting software was used to estimate a "smooth curve" fit to the remaining observations (Thoning et al., 1989; http://www.esrl.noaa.gov/gmd/ccgg/mbl/crvfit/crvfit.html). The following fit parameters were used in CCGCRV: short-term cutoff filter=80 days, long-term cutoff filter=667 days, npoly=3, nharm=4. Data were fit iteratively, continually excluding outliers greater than $\pm2\sigma$ from the smooth curve fit until no more outliers could be removed.

10 A multi-species filter was also applied, so that if either CO_2 or CH_4 were outliers from the smooth curve, then both observations were omitted. The MWO flask data were fit using a similar approach (but only using nighttime flask data to prevent potential contamination due to upslope winds). For MWO, the following fit parameters were used in CCGCRV: short-term cutoff filter=30 days, long-term cutoff filter=667 days, npoly=3, nharm=4, and the data were fit iteratively excluding outliers as described above. The full datasets, selected data and "smooth curve" results are

15 shown in Figure 3 in the main text and a comparison of the final smooth curve results for each site is shown in Figure 4 (top panels). Figure S10 shows the same results with uncertainty estimates calculated as described in Section 6.2 of the main text. Overall, we have achieved a reasonable level of convergence between the background estimates for three sites with very different variability in CO_2 and CH_4 mole fractions. A metric of success exhibited by our results is that the background reference curve estimates agree within $\sim\pm1$ ppm CO_2 and $\sim\pm10$ ppb CH_4 for the

20 marine sites (LJO and SCI) and continental sites (MWO and VIC, see Figures 4 and S10).

4) Uncertainty due to Nafion drier permeability

The laboratory experiments described here were performed at the Scripps Institution of Oceanography to estimate the uncertainty in the water vapor correction due to bias caused by the permeation of CO_2 and CH_4 across the membrane of the Nafion drier. We measured two dry standard tanks for 1200 seconds each, alternating one

25 directly after the other. The measurement system setup was identical to those used at our field sites, with a Nafion dryer located upstream of the instrument. The water vapor concentrations at the start of the measurements were 0.095%, reflective of the Nafion dryer conditions during the ambient air measurements just prior to this experiment. As the measurements continued, the Nafion dryer gradually dried out, which reduced the permeation of CO_2 and CH_4 across the membrane. This effect leads to a small increase in the CO_2 and CH_4 levels measured on the Picarro

30 analyzer (Figure S6). In this experiment, we assume that other factors such as instrument drift are negligible over the duration of this experiment (approximately 16 hours).

The uncertainty due to the Nafion permeation effect is derived from the slope of measured CO_2, CH_4 concentrations against water vapor concentrations during our experiment, as shown in Figure S6. CO_2 concentrations are found to decrease at a ratio of -1.15 ppm per 1% change in water vapor concentration in the range

35 of 0 to roughly 0.095%, while CH_4 concentrations are found to be small at a ratio of 0.029 ppb per 1% water vapor

concentration change within a range of 0.03 to roughly 0.095%. As the water vapor concentrations in our field measurements lie within a range of 0.01±0.001%, we estimate the potential bias introduced by the 0.001% range in water vapor concentrations to be -0.0115 ppm for CO_2 and 0.000029 ppb for CH_4.

Note that while the permeability of CH_4 through the Nafion membrane is shown to change dramatically in water vapor concentrations lower than 0.03%, this effect can be effectively ignored for our purposes considering the range of water vapor concentrations measured at our sites.

Also, since the relationship between permeation through the Nafion membrane and water vapor concentration has been established, it is also possible to correct for this bias and report an uncertainty on the confidence of our understanding of this relationship. This correction may potentially be added in the future, which would further reduce the uncertainties due to this effect.

6
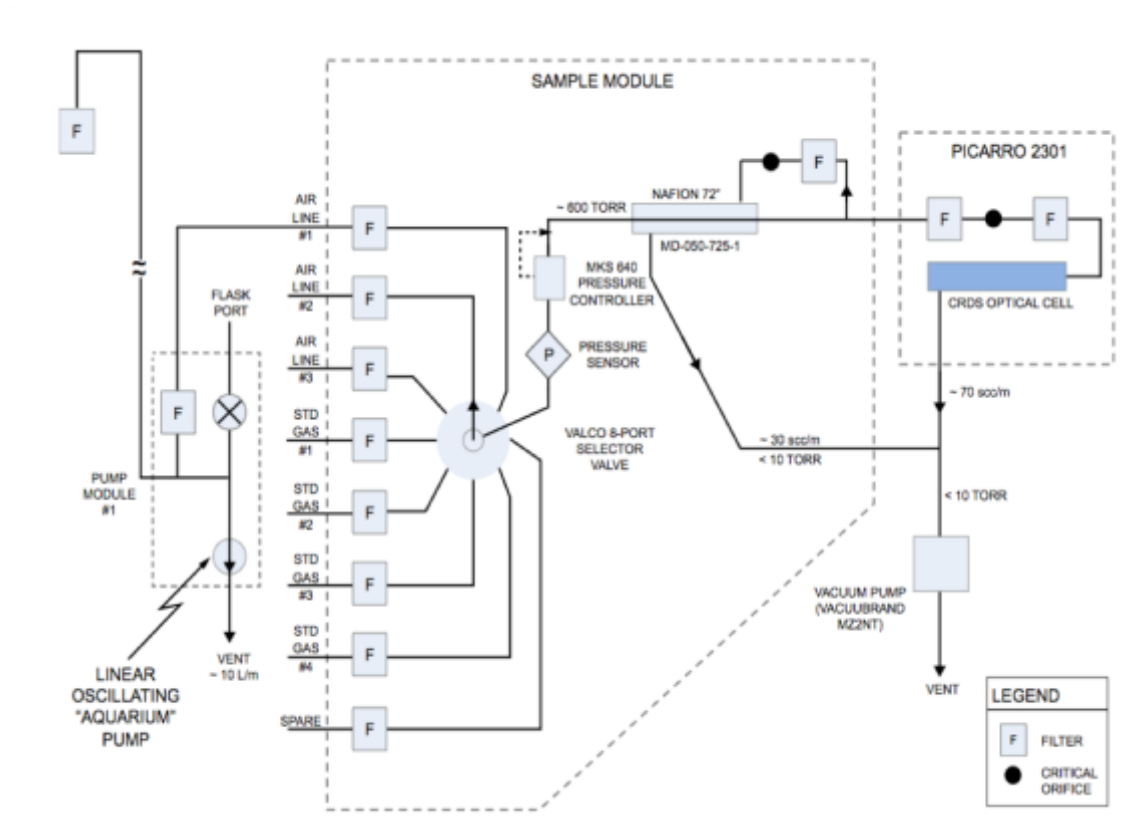
Figure S1. Diagram showing the standard gas-handling configuration for an Earth Networks greenhouse gas monitoring tower sampling from a single air inlet (see text). Figure and caption adapted from Welp et al. (2013).
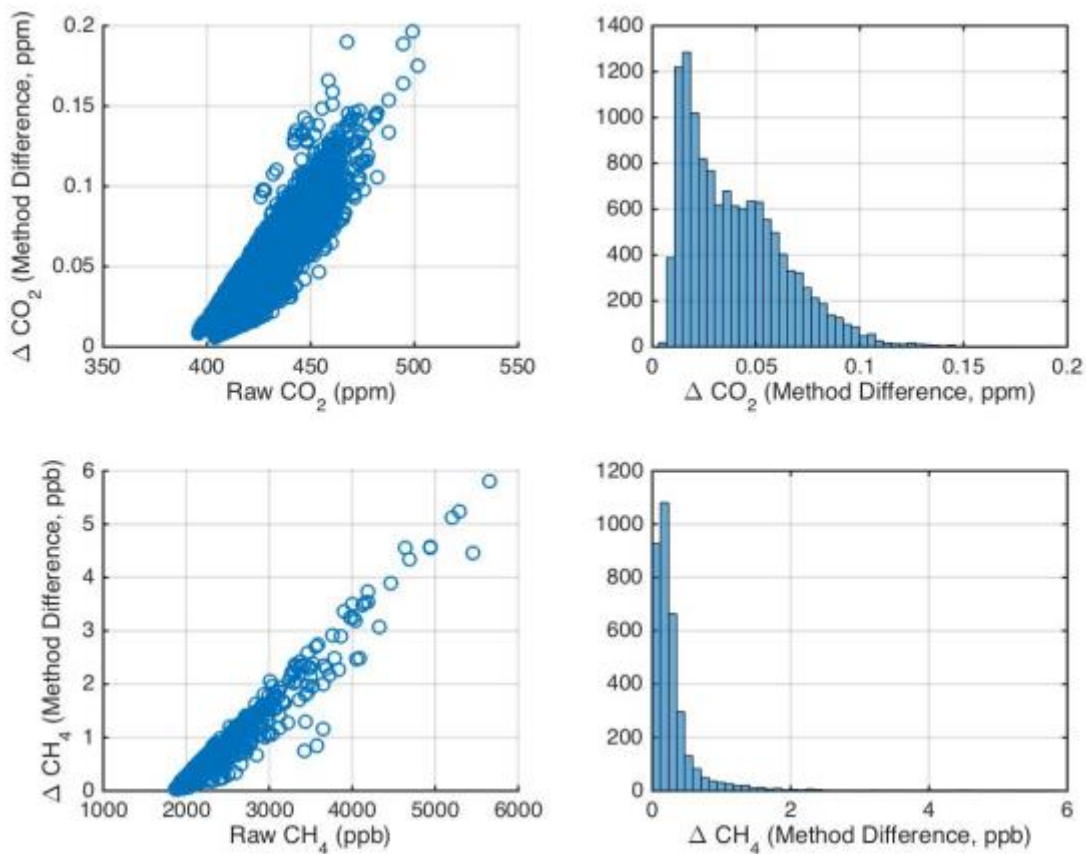
Figure S2. "Alternate Calibration Method" plotted versus uncorrected CO_2 and CH_4 air sample measurements for the LJO site. A limited number of measurements of a high mole fraction CO_2 and CH_4 standard were available at the LJO field site between October 2015 and March 2016. "Method Difference" indicates the difference in the correction of the air data using a single-point relative to a 2-point calibration. Histograms show that the uncertainty associated with using a single-point calibration is <0.2 ppm CO_2 and <4 ppb CH_4 for air measurements collected during this period.
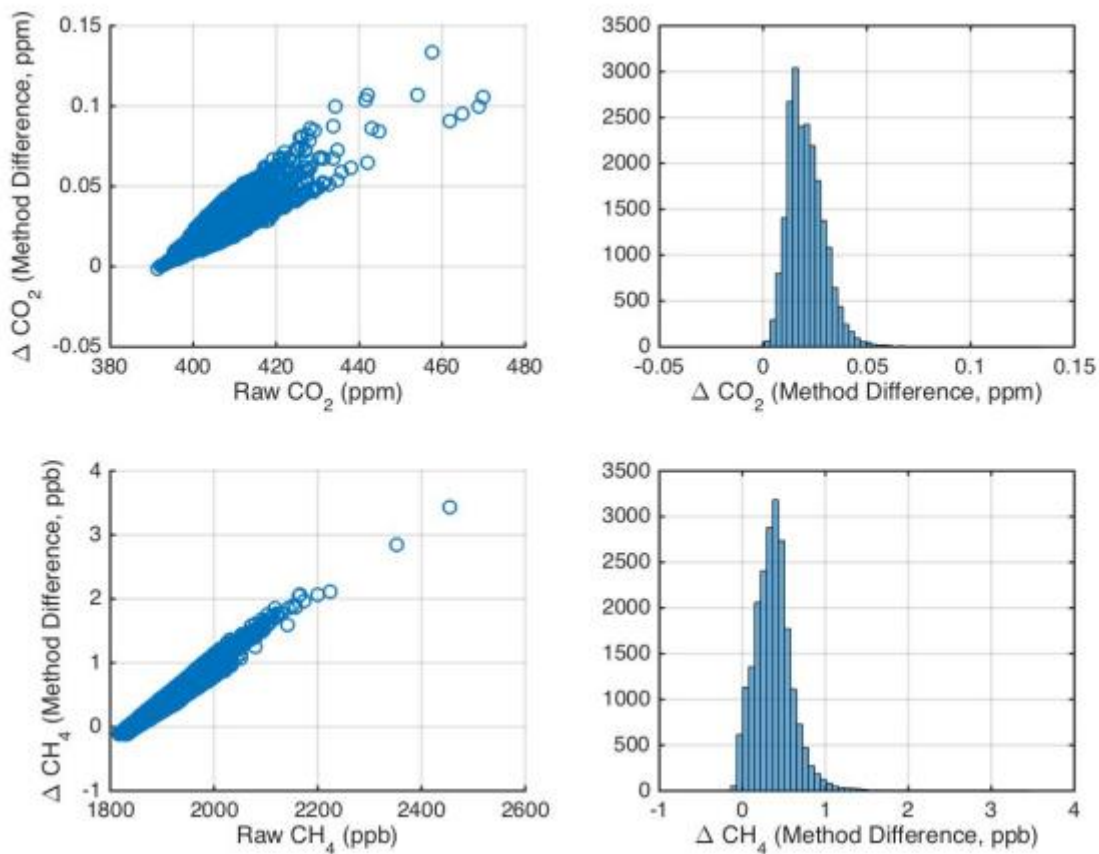
Figure S3. Same as Figure S2, except for the VIC site, which also had limited measurements of a high mole fraction CO_2 and CH_4 standard available at the time of this study. Histograms show that the uncertainty associated with using a single-point calibration is <0.15 ppm CO_2 and <4 ppb CH_4 for the majority of the air measurements collected during this period. Overall, the corrections are slightly smaller because the CO_2 and CH_4 enhancements at VIC are smaller relative to LJO.
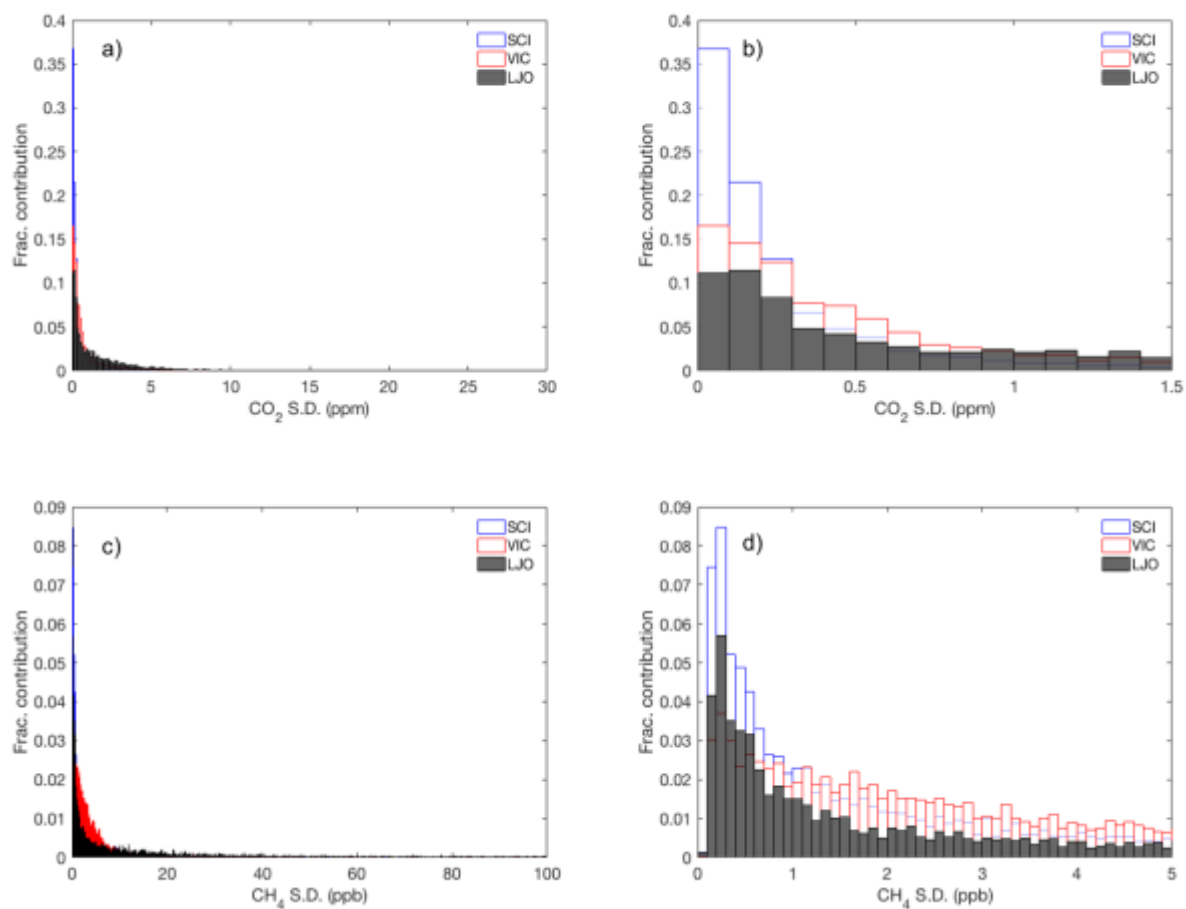
Figure S4: Histograms of the standard deviation of hourly CO_2 (panels *a and b*) and CH_4 (panels *c and d*) observations from the SCI (blue), VIC (red), and LJO (grey) sites. Left panels show histograms for all data. Right panels show the same data with the x-axis truncated for values >1.5 ppm CO_2 and >5 ppb CH_4.

5
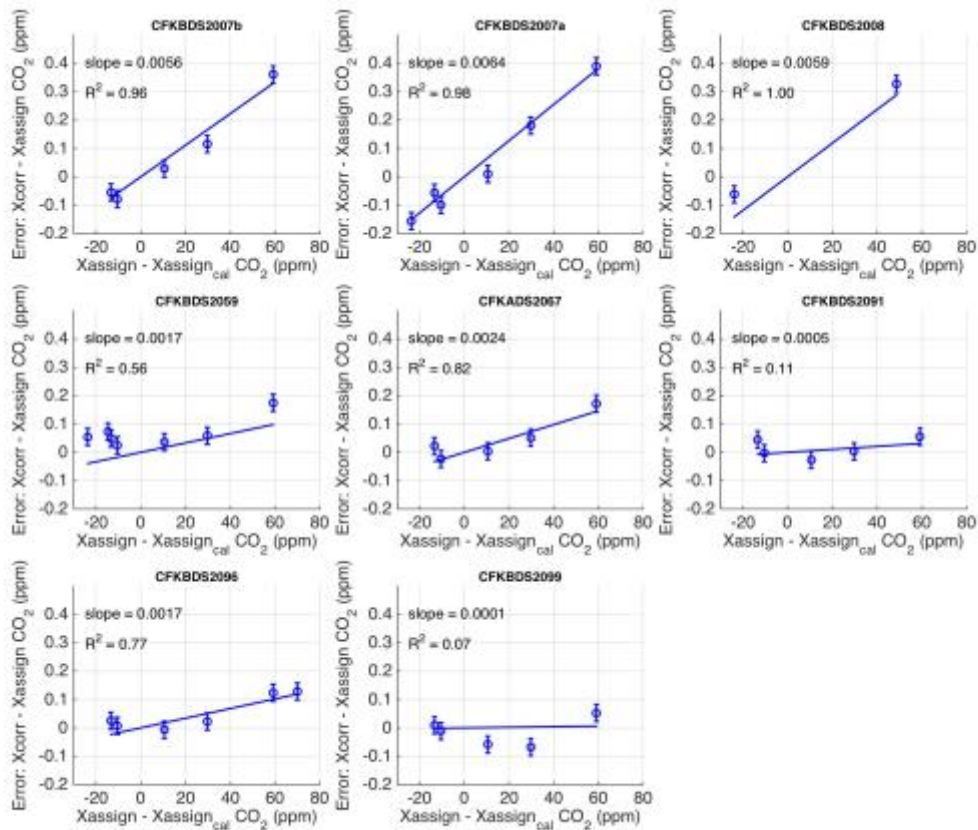
Figure S5. Estimates for epsilon (ε), the slope component of the extrapolation uncertainty (U_{extrap}) for CO_2 based on measurements from seven Picarro CRDS analyzer units. All calibrations were performed on the same suite of tanks at the NOAA/ESRL calibration laboratory. *Xassign$_{cal}$* is the assigned value of the calibration standard on the WMO scales (in this case the tank with CO_2 value closest to 400 ppm). The calibration standard was used to correct the uncorrected measurements of other standard gases using Eq. 2 in the main text. *Xassign* is the assigned value of the other standard tanks on the WMO scale (i.e., the span tanks with varying concentrations), and *Xcorr* is the calibrated data. The slope of the residual (*Xcorr – Xassign*) is plotted as a function of the concentration difference between each of the standard tanks and the assigned calibration tank (*Xassign$_{span}$ – Xassign$_{cal}$*), and is a measure of ε. All tanks were calibrated on the WMO/NOAA scales at the NOAA/ESRL laboratory. All Picarro analyzers shown here are similar models to those deployed in the LA network. The same suite of standard tanks was run on each analyzer prior to deployment for various field campaigns (with the exception of CFKBDS2008). CFKBDS2007a and CFKBDS2007b indicate two different calibrations of the same analyzer. All regressions are forced through zero. Error bars show the scale reproducibility (1σ) for the tank values reported by NOAA/ESRL (0.03 ppm CO_2; *Andrews et al.*, 2014 and *B. Hall*, personal communication).
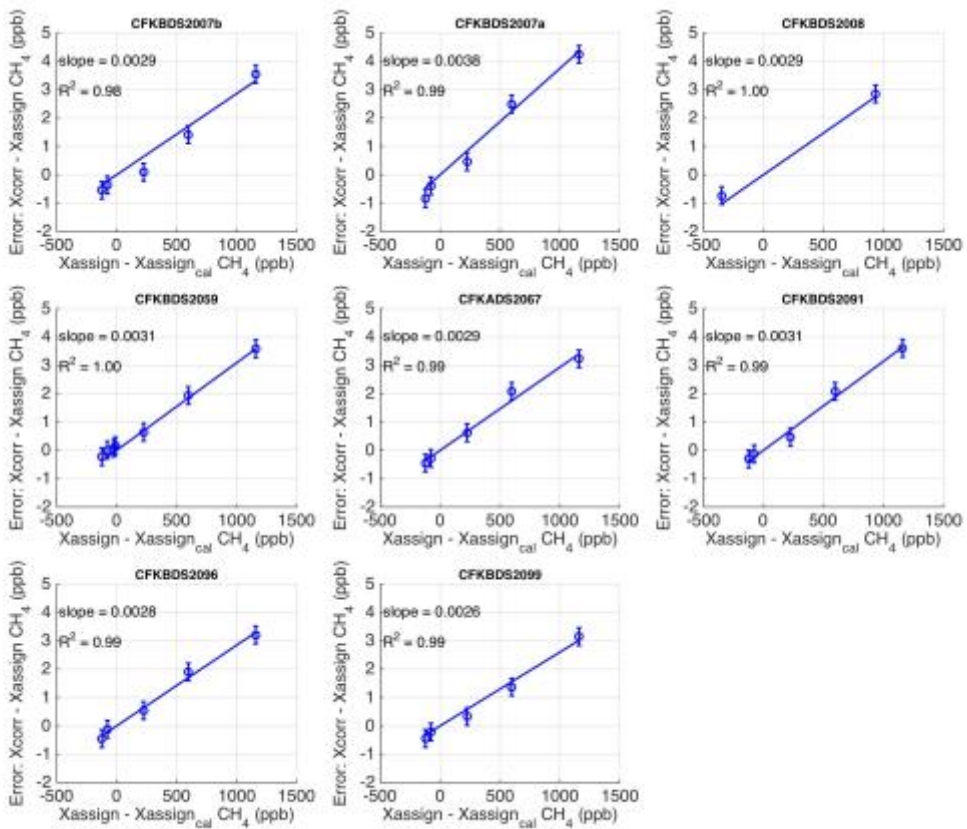
Figure S6. Estimates of epsilon (ε), the slope component of the extrapolation uncertainty (U_{extrap}) for CH$_4$ using the same suite of tanks as in Figure S4. All regressions are forced through zero. Error bars show the scale reproducibility (1σ) for tank values reported by NOAA/ESRL (0.31 ppb; CH$_4$ Andrews et al., 2014).

5
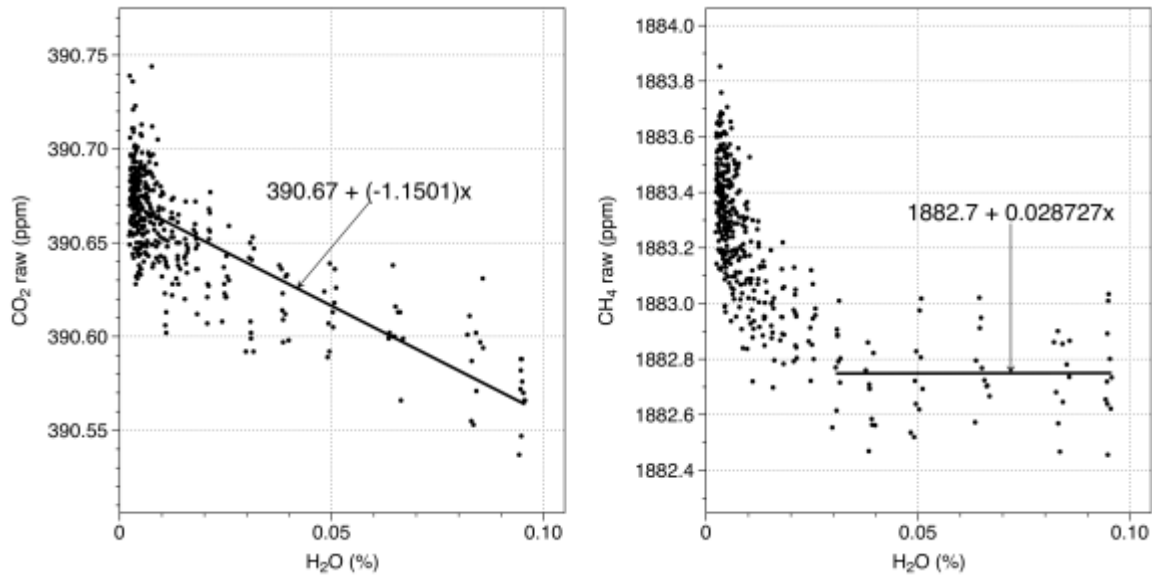
Figure S7. Results of Nafion permeation experiment. A slight increase in the measured CO_2 and CH_4 levels (shown here as uncalibrated CRDS readings) was found as the Nafion membrane dried out, leading to less permeation across the membrane throughout the experiment. We assume that these changes in the measured concentrations are not due to any other factors such as instrument drift. For simplification, only one of the two tanks measured during the experiment is shown. For CO_2, the relationship between measured concentrations and water vapor concentration is derived for the complete water vapor concentration range. For CH_4 we only consider the range of 0.03 to 0.095% H_2O since the permeation effect is different at lower water vapor concentrations, and the water vapor concentration for the field measurements in our network are within the 0.01±0.001% range.

13
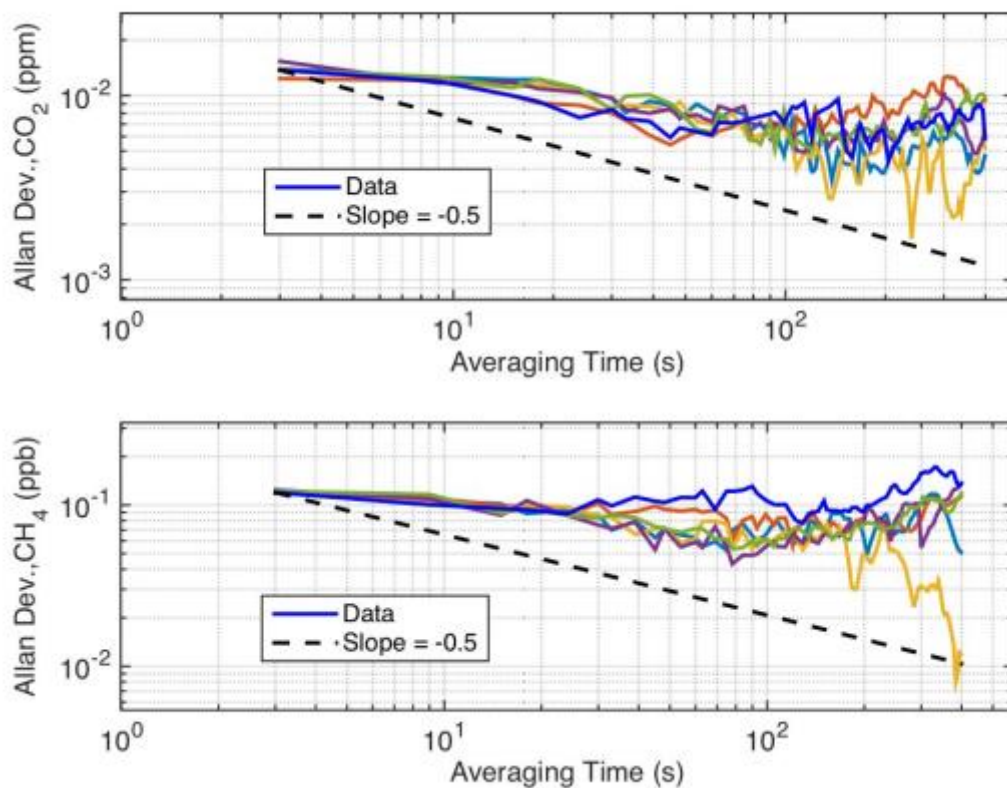
Figure S8. Allan deviation analysis from a subset of the daily calibration runs collected on the LJO analyzer during January 2016 (every 5th run is plotted for clarity). The results show that the characteristics of the noise in the analyzer vary with time. In general, the results for the calibrations are not all the same and do not fit a white-noise profile (indicated by the dashed line with slope of -1/2), indicating correlation in the noise at various longer time scales.

5
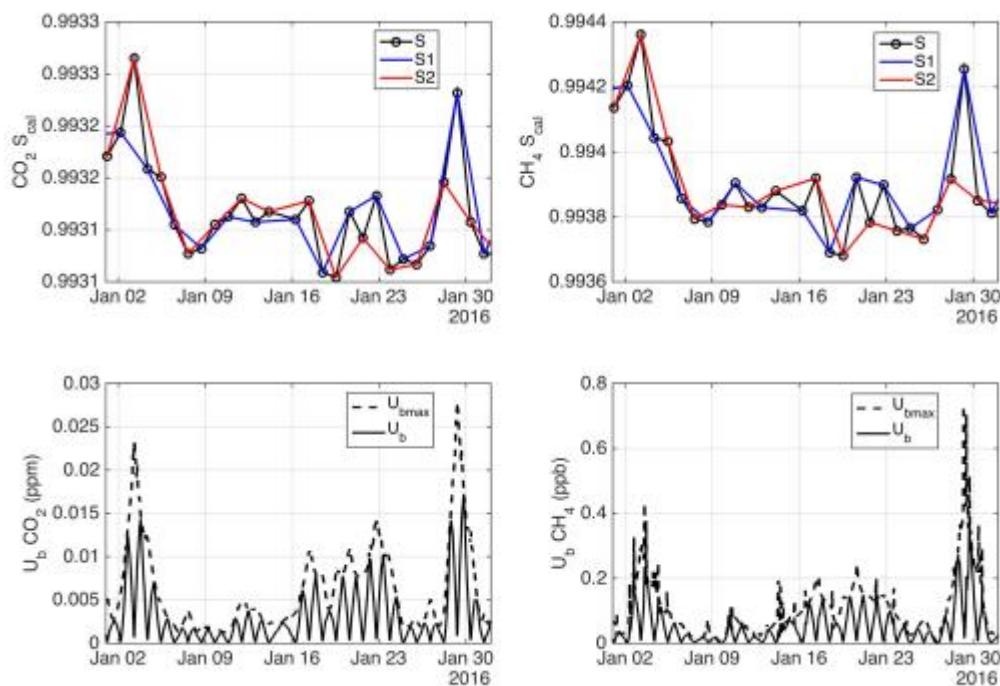
Figure S9. Example showing three possible time series of Picarro sensitivity for the standard tank measurement (upper panels) and the impact on estimates of calibration baseline uncertainty (lower panels). Results are shown for LJO data collected during January 2016. Upper panels: S is the sensitivity of the standard at the times when the reference tank was sampled (black points), which is calculated as the ratio of the measured analyzer mole fraction for the reference gas and the tank's assigned value (see text). The sensitivity of the standard is linearly interpolated in time, as shown by the black lines for CO_2 (left) and CH_4 (right). The traces, labelled S1 (blue lines) and S2 (red lines), show two alternate realizations of the analyzer sensitivity based on different interpolation methods (e.g. interpolating at points halfway between the sequential standard tank measurements, leaving out every other point). Lower panels: Calibration baseline uncertainty (U_b and $U_{b_{max}}$) calculated for CO_2 (left) and CH_4 (right). U_b reduces to zero at the times when the calibration gas was run because the tank value is measured at that time.

15
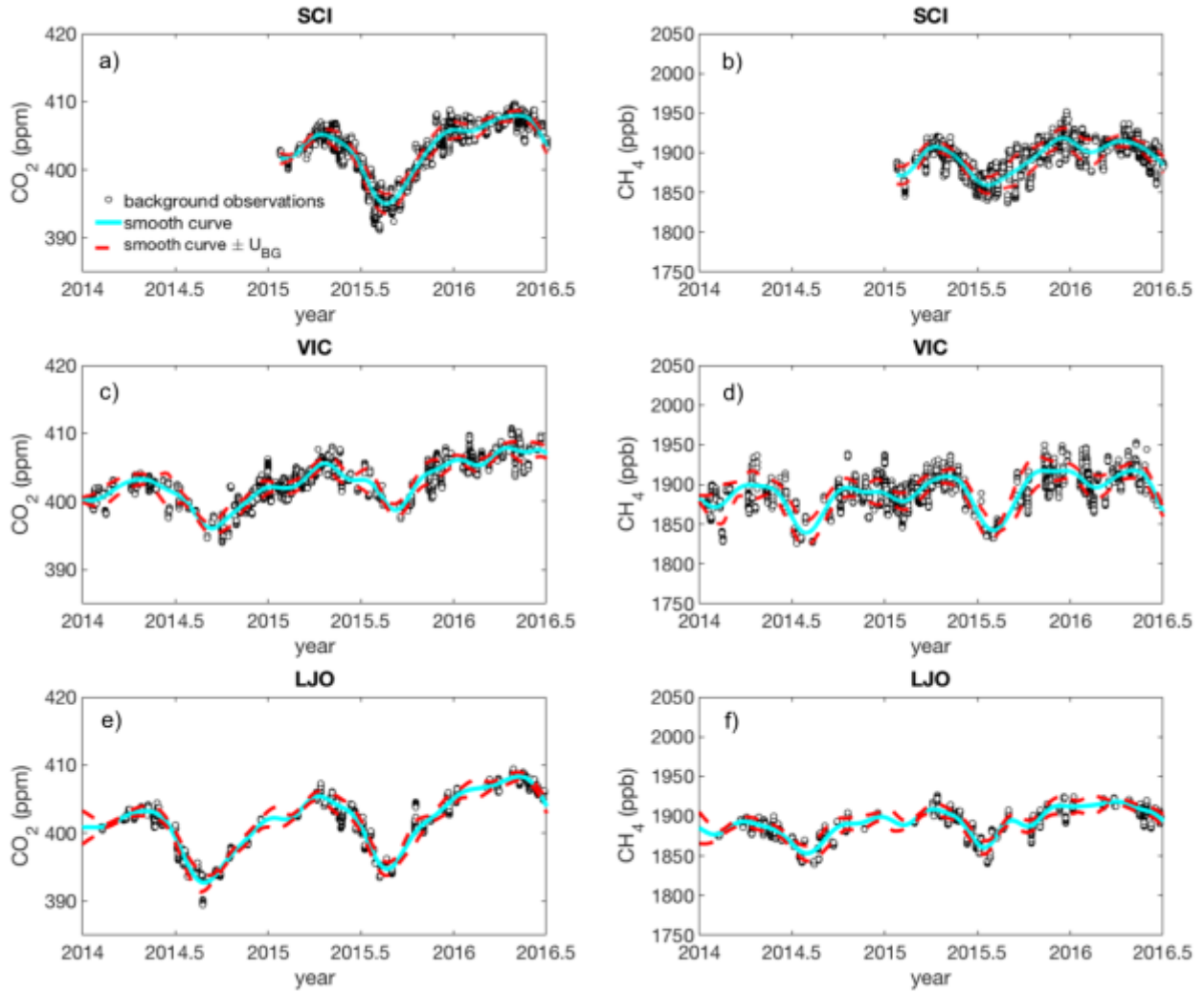
Figure S10. Background observations (black circles), smooth curve estimates (cyan lines) and uncertainty estimates (red dashed lines) for San Clemente Island (panels *a-b*), La Jolla (panels *c-d*), and Victorville (panels *e-f*) for CO_2 and CH_4. During 2015, the annual average uncertainty in the SCI smooth curve estimate was 1.4 ppm CO_2 and 11.9 ppb CH_4.
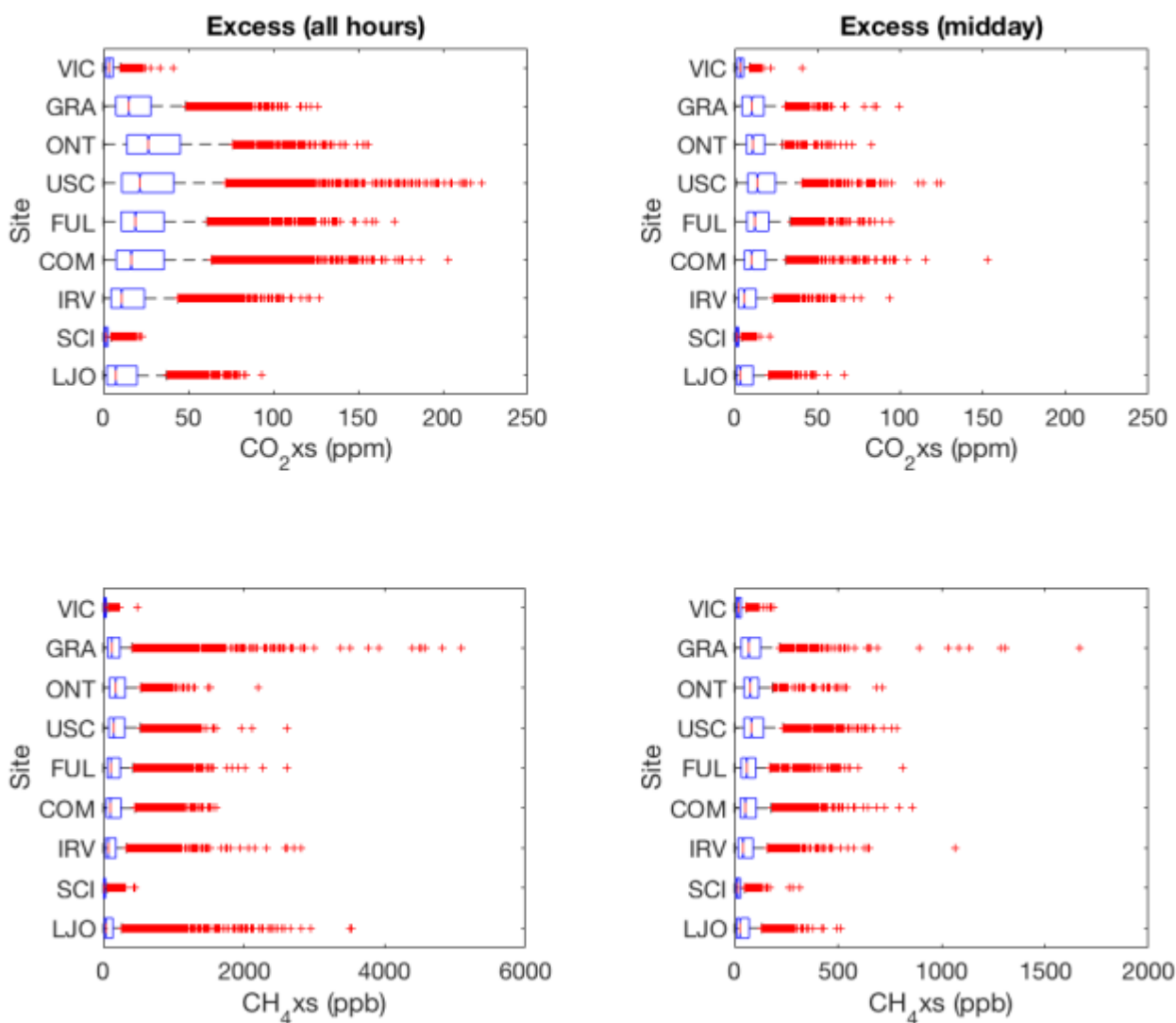
Figure S11: Boxplot of enhancements (CO_2xs and CH_4xs) in the LA megacity during 2015. Results for CO_2xs (upper panels) and CH_4xs (lower panels) are shown for all hours (left panels) and mid-afternoon hours (12-16:00 LT, right panels). The sites are arranged by latitude from north to south (top to bottom): Victorville (VIC), Granada Hills (GRA), Ontario (ONT), University of Southern California (USC), Fullerton (FUL), Compton (COM), Irvine (IRV), San Clemente Island (SCI) and La Jolla (LJO). Boxes outline the 25th and 75th percentiles of the sample data, respectively and red vertical lines show the median value at each site. The maximum whisker length is specified as 1.0 times the interquartile range (i.e. $[q_3 + w*(q_3 - q_1)]$ and $[q_1 - w*(q_3 - q_1)]$, where q_1 and q_3 are the 25th and 75th percentiles and w=1.0). Red pluses (+) indicate enhancements greater (or less than) the maximum whisker length to show the full range of variability. (Note: Results for the ONT site include observations for September –December 2015 only, while all other results are annual averages. Results from the USC site are shown for the G2401 analyzer only).

Table S1. Automated flagging and filtering criteria applied to the CRDS measurements using the GCWerks software. Data meeting the filter criteria are flagged to identify periods when the CRDS analyzer may be subject to large errors and greenhouse gas observations collected during such periods were excluded from further analysis. Flags and filters are applied to high-resolution (roughly 2.5 second) CRDS readings.

Symbol	Filter name	Frequency	Criteria
P	Cavity pressure[1]	3-5 sec	Cavity pressure out of range (139.9-140.1 Torr)
T	Cavity temperature	3-5 sec	Cavity temperature out of range 44.98-45.02 °C
W	High water	3-5 sec	Water value too high (>10%)
C	Cycle time[1,2]	3-5 sec	Cycle time too high (>8 seconds/cycle)
S	Standard deviation[3]	Varies	For measured compound or water only
			Calibration standards only: applies to 20-min window, filters values $>3\sigma$
			Air data only: applies narrow 2-minute moving window, filters values $>10\sigma$

(1) Indicates the filter contains a user defined or specified value within GCWerks.

(2) Cycle time is defined as the time between subsequent trace gas measurements. Note: For periods in which a data point is separated from adjacent points by more than the specified maximum cycle time, all 3 points will be filtered. For Los Angeles, the default maximum for cycle time filter is 8 seconds. Representatives from Picarro Inc. recommend the cycle time value should not normally exceed 5 seconds (C. Rella, *personal communication*).

(3) For each measured compound (and water) any data points outside of the user-defined number of standard deviations are automatically filtered. The filter is applied recursively until no more points are filtered in each mean. For calibration tank measurements, the remaining 10-minute period (after the initial 10 minute rejection period) is filtered at once (i.e., no moving window) using a 3σ SD filter. For air data, a narrow 2-minute moving window is used to only filter extreme outliers ($>10\sigma$ SD, default) that may result from instrument errors. The moving windows overlap 1-minute, and the center 1-minute is filtered, while ends (first and last 30 seconds of each air measurement) are not filtered.

Table S2. Estimates of ε, the slope component of U_{extrap}, the uncertainty due to the single-point calibration strategy, based on laboratory experiments and field data. Two values are from analyzers deployed at the LJO and VIC sites using limited measurements of a high mole fraction tank deployed in the field. Additional estimates of ε were collected from laboratory calibrations at NOAA/ESRL using CRDS analyzers with similar model numbers (see Figures S4 and S5). Two different sets of calibration results are available for one of the analyzers (CFKBDS-2007a and -2007b).

no.	Analyzer model	CO_2 slope (ε) (ppm/ppm)	R^2	CH_4 slope (ε) (ppb/ppb)	R^2
1a	CFKBDS-2007a	0.0064	0.98	0.0038	0.99
1b	CFKBDS-2007b	0.0056	0.96	0.0029	0.98
2	CFKBDS-2008	0.0059	n/a	0.0029	n/a
3	CFKBDS-2059	0.0017	0.56	0.0031	1.0
4	CFKADS-2067	0.0024	0.82	0.0029	0.99
5	CFKBDS-2091	0.0005	0.11	0.0031	0.99
6	CFKBDS-2096	0.0017	0.77	0.0028	0.99
7	CFKBDS-2099	0.0001	0.07	0.0026	0.99
8	LJO	0.0027	n/a	0.0012	n/a
9	VIC	0.0018	n/a	0.0060	n/a

Table S3. Estimates of the uncertainty in the single-point calibration method based on laboratory experiments and limited measurements of high concentration standards deployed in the field. Corrections to the air data estimated assuming a 100 ppm CO_2 and 4 ppm CH_4 enhancement above the "near ambient" calibration standard and various estimates for ε.

	CO_2 slope (ε) (ppm/ppm)	CH_4 slope (ε) (ppb/ppb)	CO_2 correction given a 100 ppm enhancement (units: ppm)	CH_4 correction given a 4 ppm enhancement (units: ppb)
Analyzer 1 (a and b)	0.0060±0.0005	0.0033±0.0006	0.60±0.05	13.2±2.4
Analyzers 1-7*	0.0026±0.0024	0.0030±0.0002	0.26±0.24	12.0±0.8
Analyzers 1-9*	0.0025±0.0021	0.0031±0.0012	0.25±0.21	12.4±4.8
LJO analyzer	0.0027	0.0012	0.27	4.8
"Alternate calibration method"**	n/a	n/a	0.2	<6

*Two different calibrations available for analyzer 1 (a and b) were averaged together first, to get a single value for analyzer CFKBDS-2007, before averaging with the other analyzers. See Table S2.

** See Figures S2 and S3.

References

Andrews, A. E., Kofler, J. D., Trudeau, M. E., Williams, J. C., Neff, D. H., Masarie, K. A., Chao, D. Y., Kitzis, D. R., Novelli, P. C., Zhao, C. L., Dlugokencky, E. J., Lang, P. M., Crotwell, M. J., Fischer, M. L., Parker, M. J., Lee, J. T., Baumann, D. D., Desai, A. R., Stanier, C. O., De Wekker, S. F. J., Wolfe, D. E., Munger, J. W. and Tans, P. P.: CO_2, CO, and CH_4 measurements from tall towers in the NOAA Earth System Research Laboratory's Global Greenhouse Gas Reference Network: instrumentation, uncertainty analysis, and recommendations for future high-accuracy greenhouse gas monitoring efforts, Atmos. Meas. Tech., 7(2), 647–687, doi:10.5194/amt-7-647-2014, 2014.

Welp, L. R., Keeling, R. F., Weiss, R. F., Paplawsky, W. and Heckman, S.: Design and performance of a Nafion dryer for continuous operation at CO_2 and CH_4 air monitoring sites, Atmos. Meas. Tech., 6(5), 1217–1226, doi:10.5194/amt-6-1217-2013, 2013.